Chapter

Vertical Axis Wind Turbine Design and Installation at Chicamocha Canyon

Luis-Fernando Garcia-Rodriguez, Juan Diego Rosero Ariza, Jorge Luis Chacón Velazco and Julian Ernesto Jaramillo Ibarra

Abstract

The use of vertical axis wind turbines (VAWT) in Colombia could tackle the energy distribution difficulties as large parts of the territory are not connected to the electrical grid. The present chapter explains how to design and select an accurate VAWT for a mountain site, (the Chicamocha's canyon) by characterizing the wind energy potential, selecting the appropriate blade's airfoil, and design its corresponding blades to obtain an accurate VAWT performance. This methodology can be used to design and allocate a VAWT for residential use, as it tackles the critical point on wind energy design and selection. It is found feasible the use of wind energy at the location where the mean year density power is 485 [W/m^2], and the DU06W200 airfoil is suggested as its aerodynamic efficiency (c_l/c_d) overcomes by 14% the commonly used NACA0018. Finally, straight blades are recommended to overcome the inertial effects of the low wind velocity at the location.

Keywords: VAWT, Colombia, wind, energy, turbine

1. Introduction

There is a need of developing wind energy solutions capable to adapt fluctuating flow resources to have a diversified energy portfolio for the energy demand in Colombia [1]. The Chicamocha's canyon topography does not allow a stable electrical grid, which difficulties the incentives for tourism and commodities at the location, and the local community needs a sustainable source of energy that does not impact the environment. Therefore, this work assembles the feasibility for installing Vertical Axis Wind Turbines (VAWT) along with an optimal design.

The performance of a VAWT relies principally on its airfoil and blades, which generate lift and drag forces that take advantage of the wind kinetic energy to produce torque at the shaft of the turbine. The airfoil design and selection is an important task that depends on three main topics: wind flow conditions, airfoil shape, and modeling. The Darrieus VAWT blades design are based on lift aerodynamic forces and commonly use the commercial NACA0018 airfoil, and its performance varies according to the wind velocities [2]. Claessens [3] developed the DU06W200 airfoil for VAWT turbines, which overcomes the aerodynamic performance of the NACA0018 under high wind velocities than the calculated at Chicamocha's Canyon nature. Yarusevych and Boutilier [4] analyses a similar

Reynolds number but only one angle of attack is analyzed. Therefore, Garcia Rodriguez et al. [1] complements previous studies by increasing the range of Reynolds numbers analyzed for the DU06W200 airfoil, providing further information about the aerodynamic global coefficients and analyzing the performance of both airfoils under different attack angles.

In addition, different geometrical factors related to Power Coefficient (C_p) and VAWT turbine design is presented. These parameters vary depending on the wind characteristics of the region where the turbine is installed, therefore its analysis is fundamental to determine the VAWT performance. The 3D analysis performed allows an accurate VAWT dimensions distribution, correlates literature wind speeds (between 4 and 7 m/s) works with the Chicamocha Canyon region. Finally, different the influence of the VAWT turbine blades design is analyzed, by characterizing the Savonius rotor, Troposkien design, straight blades helical blades, observing the advantages and disadvantages of each type for the conditions of the region in question.

2. Chicamocha's canyon wind energy characterization

The Chicamocha's canyon national park, known as "PANACHI", monitor constantly the wind velocity at the canyon to control the cableway safety installed at the location. The administration of the park provided to [1] research the historical data from the year 2009 up to 2012. The wind velocity magnitude is characterized at three different locations: the two highest points of the location ("Mesa de Los Santos" and "PANACHI") and the river point.

The wind energy potential of the canyon is analyzed by using the mass conservation principle Eq. (1):

$$\frac{dm}{dt} = \rho * A * U \tag{1}$$

where ρ is the air density, U the velocity and A is the swept area. Then, the wind energy potential, P, can be expressed as kinetic energy per time unit as Eq. (2):

$$\frac{P}{A} = \frac{1}{2} * \rho * U^3 \tag{2}$$

Manwell et al. [5] establishes how significant the wind energy potential is at a selected location (**Table 1**).

The annual average wind speed and wind power density of the three locations are shown in **Table 2**. Garcia Rodriguez et al. [1] concludes that the suitable VAWT location is at Chicamocha's river due to its high wind speed, 6.9 [m/s], and the critical point is found at "Mesa de Los Santos" location.

$P/A < 100\ W/m^2$	Poor
$P/A \approx 400\ W/m^2$	Good
$P/A > 700\ W/m^2$	Excellent

Table 1.
Wind power potential criterion [5].

Place	Annual average wind speed [m/s]	Standard deviation	Annual average wind power density [W/m^2]
"Mesa de los santos"	5.9	0.736	306.188
Chicamocha's River	6.9	1.084	485.115
"PANACHI"	4.3	0.536	86.643

Table 2.
Wind power potential at Chicamocha's canyon [1].

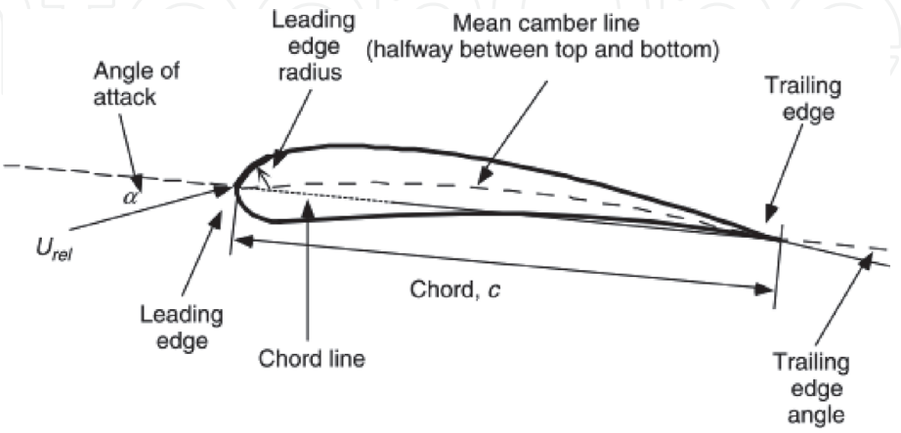

Figure 1.
Aerodynamics nomenclature [5].

3. VAWT aerodynamics

3.1 Aerodynamic airfoil and blades

An airfoil is identified using its aerodynamic parameters [5] as shown in **Figure 1**. The mean curve line is the focus midway points between the upper and lower surfaces of the airfoil. While the straight line connecting the leading and trailing edges is called the airfoil chord line, and the distance from the leading edge to the trailing edge measured along the chord line is known as the aerodynamic airfoil's chord (c). Finally, the angle of attack, α, is defined as the angle between the relative wind (U_{rel}) and the chord [6].

3.2 Lift, drag, and dimensionless parameters

The airflow over an airfoil produces a force distribution on the surface. The flow velocity increases over the convex surface resulting in lower average pressure on the "suction" side of the airfoil compared to its concave "pressure" side. Meanwhile, the viscous friction between the air and the surface of the airfoil slows the airflow to a certain point near the surface [6].

There are three forces of vital importance for aerodynamic analysis as seen in **Figure 2**, which are:

- The lifting force goes in the perpendicular direction to the incident airflow. The lift force is a consequence of the pressure differential generated between the upper and lower surfaces of the airfoil.

- Drag force is the tangential component and occurs due to friction forces on the surface of the airfoil

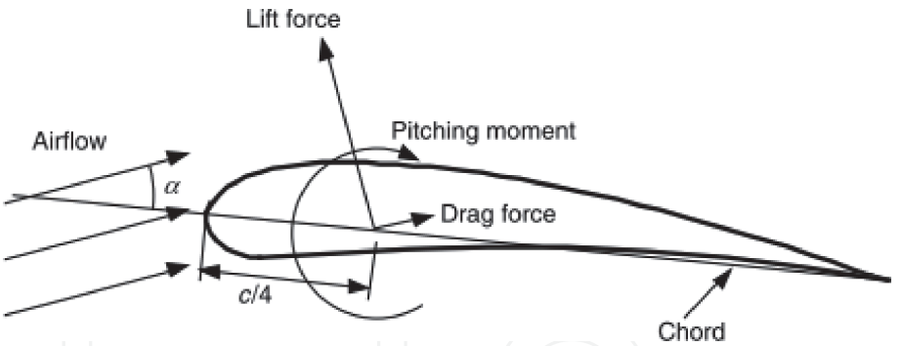

Figure 2.
Forces and moments in an aerodynamic section, an angle of attack; c, chord. The direction of positive forces and moments is indicated by the direction of the arrow [5].

- Pitch moment is defined around a perpendicular axis to the cross-section of the airfoil.

- Lift and drag coefficients: The lift and drag forces (per unit length of the blade) are usually expressed as a function of two coefficients CL and CD in Eq. (3) and Eq. (4) respectively.

$$C_L = \frac{L/l}{\frac{1}{2}\rho U^2 c} \tag{3}$$

$$C_D = \frac{D/l}{\frac{1}{2}\rho U^2 c} \tag{4}$$

where c is the chord of the blade. The lift and drag coefficients are expressed as a function of the angle of attack (γ). **Figure 3** shows the typical coefficients of wind turbine blades. Note that the CL coefficient grows approximately linearly with the angle of attack, while CD remains at a low value. For angles of attack greater than 13°, CL decreases while CD grows rapidly, and the blades go into loss.

The power output is produced through the lift force generated on the airfoil surface. As the turbine rotates, the airfoils encounter an incident wind velocity that is the vector summation of the surrounding flow velocity and the turbine rotation **Figure 4** [8].

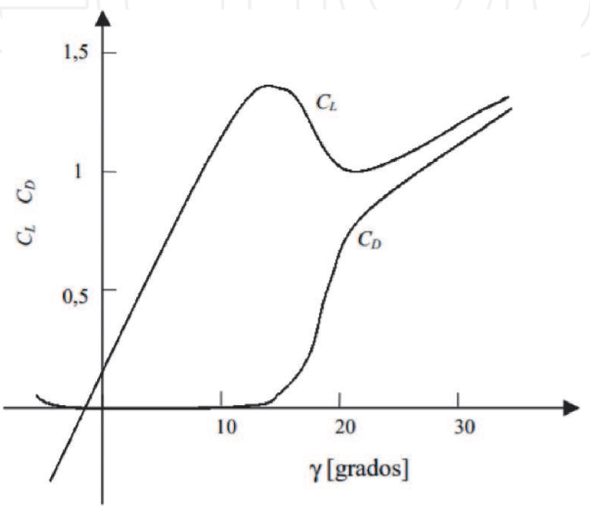

Figure 3.
Coefficients of lift and drag of a blade [7].

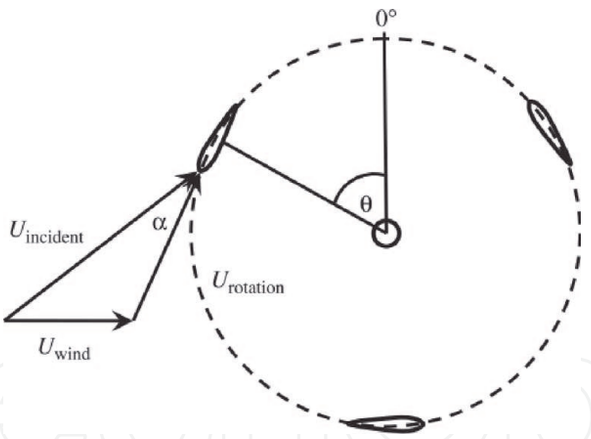

Figure 4.
Vertical axis wind turbine principle of operation. α is the relative angle of attack of the incident flow velocity U incident, and e is the angle of rotation [8].

3.3 Reynolds number (Re)

Defines the characteristics of flow conditions Eq. (5):

$$Re = \frac{UL}{v} = \frac{\rho UL}{\mu} = \frac{Inercial\ Force}{Viscous\ Force} \tag{5}$$

where μ is the fluid viscosity, U and L are the velocity and length that characterize the flow scale. These can be the inflow velocity of the flow, U_{wind} and the chord length of an airfoil. In addition to the Reynolds number of the flow conditions, the Reynolds number based on the chord c is also important.

Brusca et al. [9], defined the Reynolds number based on the chord (Re_c), and can be expressed as follow the Eq. (6)

$$Re_c = \frac{cw}{v} \tag{6}$$

where c is the chord, w is the air's relative velocity to the aerodynamic surface and v is the air's kinematic viscosity. The c can be expressed as a function of the solidity (σ) of the turbine Eq. (7):

$$c = \frac{\sigma Cp_{max}}{Nb} R \tag{7}$$

where σ is the solidity, Cp is the Power Coefficient, Nb is the number of blades and R is the turbine's radio. Therefore, Re_c is directly proportional to σ and Cp as follow Eq. (7):

$$Re_c = \frac{\sigma Cp_{max} Rw}{Nbv} \tag{8}$$

The Reynolds number strongly influences the power coefficient of a vertical-axis wind turbine. Furthermore, it changes as the main dimensions of the turbine rotor change. Increasing rotor diameter rises the Reynolds number of the blade.

3.4 Power coefficient (*Cp*)

The turbine performance is given by the power coefficient Cp. This coefficient represents the energy produced by the turbine as part of the total wind energy that

passes through the swept area. Claessens [3], the *Cp* is represented as follow the Eq. (9):

$$C_p = \frac{P_T}{P_{wind}} = \frac{P_T}{\frac{1}{2}\rho V^3 A} \tag{9}$$

where *PT* are the total energy, ρ is the air's density, *V* is the velocity of the wind and *A* is the swept area for the turbine. Hansen et al. [10] express P_T as it shown the Eq. (10):

$$P_T = M.\omega \tag{10}$$

where *M* is the instantaneous momentum and ω is the angular velocity. Another parameter is the instantaneous moment coefficient (C_m) indicating the torque generated by the blades in the Eq. (11):

$$C_m = \frac{M}{\frac{1}{2}\rho V^2 AR} \tag{11}$$

3.5 Solidity and tip speed ratio

The solidity and Tip Speed Ratio of the turbine are directly related with the C_p as will be seen in this section, therefore, they are crucial in the design of VAWT. With the correct relation of these, it can obtain the maximum C_p. These parameters are shown below.

3.5.1 The solidity of the turbine (σ)

The solidity of the turbine (σ) it can see in Eq. (12), is defined as the developed surface area of all blades divided by the swept area [11].

$$\sigma = \frac{Nc}{R} \tag{12}$$

σ has a strong influence on VAWT performance. High solidity machines reach optimum efficiency at a low Tip Speed Ratio (λ) and efficiency drops away quickly on either side of this optimum [12].

A low solidity results in less total blade area, therefore, the blade is lighter. This benefits wind turbine performance as higher rotation speeds can be reached [6].

Paraschivoiu [11] establishes that a maximum *Cp* value rise a pick in a range of σ between 0.3 and 0.4, and then, it decreases. This peak value is not higher than *Cp* in the proposed solidity of 0.2. This statement is closely linked to the result obtained by [13], which proposes through its computational tool an optimal value of σ between 0.25 and 0.5.

In **Figure 5**, it can observe when the solidity is increased from 0.05 to 0.2, the static torque coefficient will increase by a factor of approximately 4 for an H-Darrius wind turbine. Therefore, for a high solidity, the turbine has a self-starting capability, because it has a higher static torque coefficient than the low solidity turbines [15].

Increasing *σ* can decrease the negative *Cp* region (i.e, when the turbine is not self-starting) and even make the *Cp* values completely positive for solidity values of 0.6 or more [3]. However, the result of this is very large blades that will increase

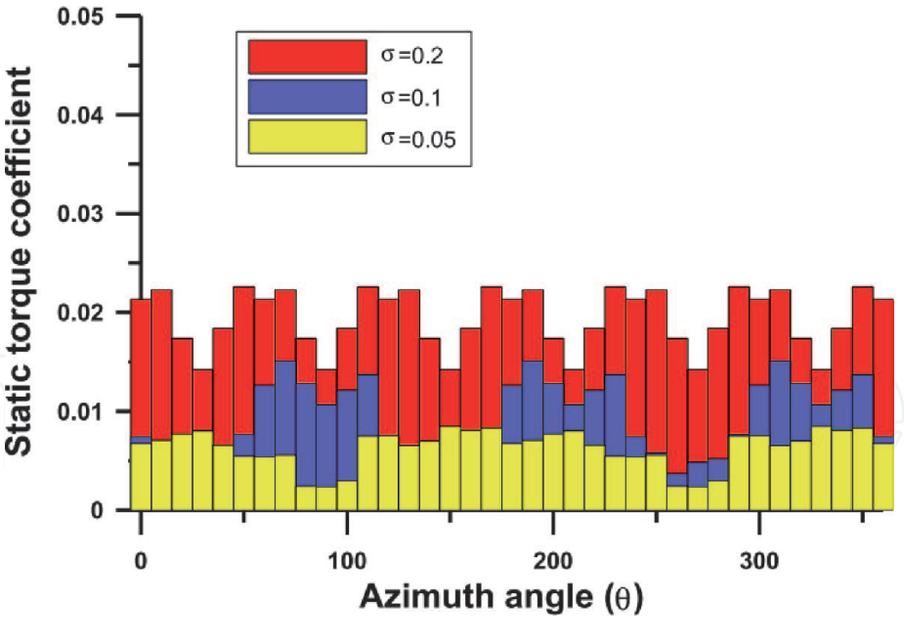

Figure 5.
Solidity effect on the static torque coefficient [14].

their manufacturing cost, so a balance must be chosen when defining the robustness of the turbine.

3.6 Tip speed ratio (λ or TSR)

The speed ratio (λ) is a ratio between the tip blade speed (ω.R) and the freestream wind velocity, and this ratio is defined as following in Eq. (13):

$$\lambda = \frac{\omega R}{V} \tag{13}$$

In **Figure 6** it can see a relation between the azimuth angle (ɵ), the angle of attack (α), and the speed ratio (λ), this relation is as follow in Eq. (14):

$$\alpha = \tan^{-1}\left[\frac{\sin\theta}{\lambda + \cos\theta}\right] \tag{14}$$

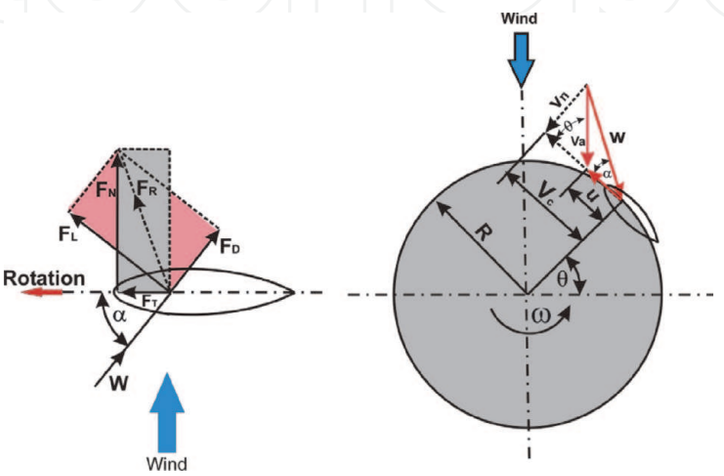

Figure 6.
Forces and velocities distribution on Darrius rotor airfoil [14].

Zouzou et al. [16] conclude in his investigation that a variable pitch VAWT has a major advantage respectively to fixed pitch VAWT in the case of high solidity rotor where the blade wake is large. That is because the pitch variation of the blade reduces flow separation and as result, the drag forces are lower. **Figure 7** shows the relationship between the drag force and the λ and the comparison between the fixed and variable pitch.

The *Cp* of a VAWT increases with an increase in the λ and reaches a peak, after which it takes a dip as larger λ are attained. **Figure 8** shows the angle of attack (α) is evaluated at different values of λ. To higher λ the value of α is smaller for a λ = 0.5 and λ = 1.5.

For VAWT λ is lower the common range is (λ = 1; λ = 5), this ranges of λ values refer to the Wind Turbine peak (Cp_{max}). **Figure 9** shows the performance of main wind turbines and some possible areas for new designs.

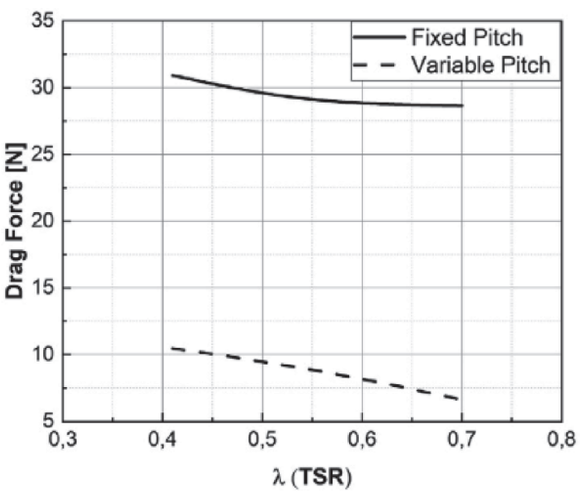

Figure 7.
The drag force of the different wind turbine configurations depends on the specific speed TSR.

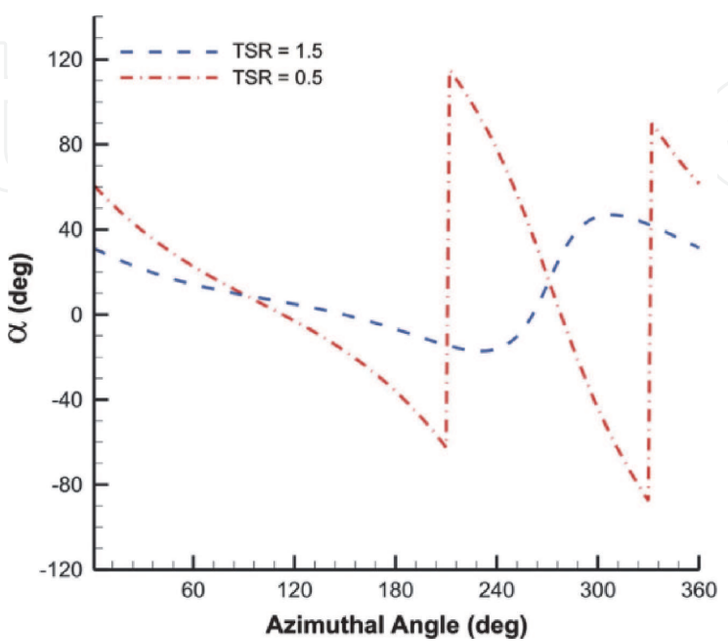

Figure 8.
Attack angle variation vs. azimuthal angle for two tip speed ratios of 0.5 and 1.5 at θp = 0° [17].

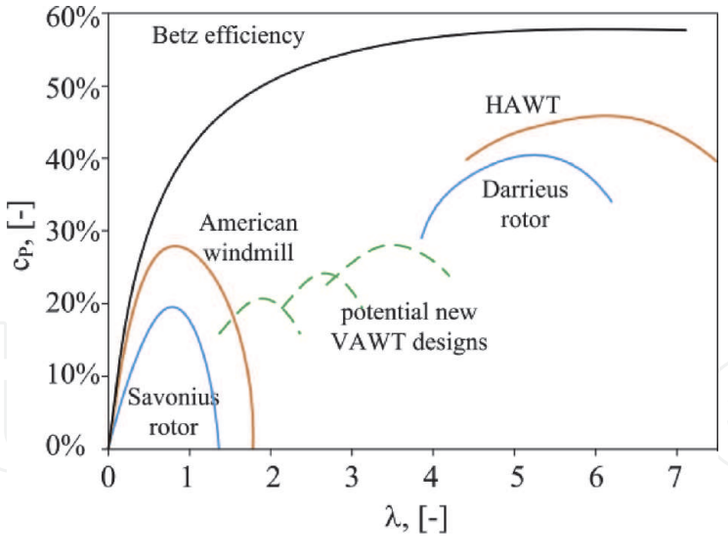

Figure 9.
Performance of main conventional wind machines and possible areas for new hybrid designs [18].

The *Cp* can be expressed in function of the λ and the *Cm*, replacing and solving Eq. (12) in (9), the *Cp* follow the Eq. (15) as follow:

$$Cp = \frac{Cm.R.\omega}{V} = Cm * \lambda \tag{15}$$

According to Posa [19] there is a relation between λ and the establishment of the flow downstream of a VAWT, this is related to the optimal distance between turbines in wind farm configurations. Establishing the downstream flow of a VAWT to its far-wake behavior takes a shorter distance at higher λ values.

4. VAWT design

VAWT design correlates geometrical characteristics of the rotor with the Power Coefficient (22) of the turbine. The influence of the main aerodynamic design parameters is compared with the operation of turbines [20]. This section presents the considerations and parameters necessary for the construction of VAWT turbines. The design procedure taking aerodynamics into account can be expressed as follows:

- Application and desired power
- Geometrical aspects
- Airfoil selection.

4.1 Application and desired power

The VAWT turbines have different applications [21] to generate electricity, pump water, purify and/or desalinate water by reverse osmosis, heating, and cooling using vapor compression heat pumps, mixing and aerating bodies of water; and heating water by fluid turbulence. Rathore et al. [22] suggests VAWT use on highways, in which vehicles travel at high speed in both directions producing an

acceleration of the surrounding wind that can be used by turbines located in the separators.

To do so, the power (P_T) required for the application is selected. This P_T is given for a particular velocity (V), area (A), density of the air (ρ), probable Power Coefficient (C_p) and efficiencies of the mechanical components (gearbox, generator, etc.) (η) as following in the Eq. (16) [6].

$$P_T = C_p\, \eta\, \frac{1}{2}\rho V^3 A \tag{16}$$

4.2 Geometrical aspects

Among the main aspects of VAWT turbines are the chord length (c), rotor height (H), rotor diameter (D), and aerodynamic airfoil (**Figure 10**).

4.2.1 Height/diameter ratio (Φ = H/D)

The relation Φ is analyzed from the turbine shape indicating the visual proportions of the turbine. On the other hand, for a fixed sweep area, low Φ values are characteristic of turbines in which optimal flow conditions are obtained in the aerodynamics airfoil, due to large diameters that increase the peripheral speed. On the contrary, high values of Φ can be related to turbines where blade efficiency is preferred [20].

The Darrieus rotor has low aspect ratios to minimize the length of the blade and the center column for a given swept area. If the Φ is increased, then the rotor speed increases (to maintain the same relative wind speed and tip speed ratio), and torque decrease if power is constant [11].

4.2.2 Chord/diameter ratio (ξ = c/D)

High ξ values indicate that chord length is increased to improve the Reynolds number, while low values relate to rotors in which the relative wind speed increases proportionally to the relative wind speed on the aerodynamic airfoil [20].

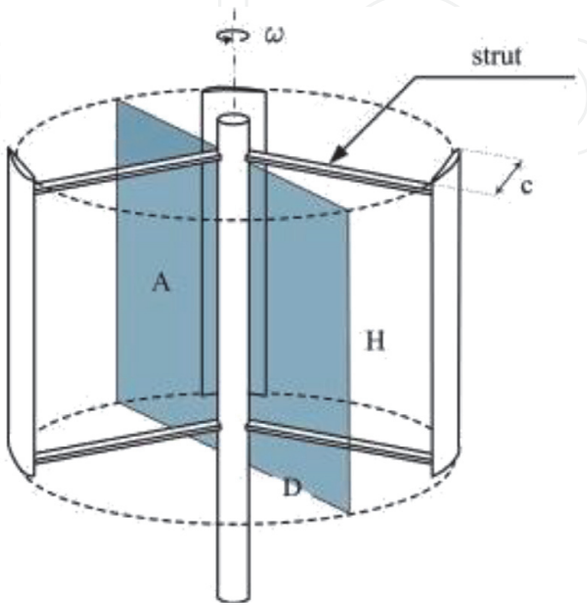

Figure 10.
Schematic view of the architecture of the Darrieus turbines [23].

4.2.3 Rotor swept area (A)

The swept area of the turbine (**Figure 10**), corresponds to the amount of air that is dragged by the turbine blades. In particular, the larger sweep areas guarantee fewer demanding limits of the turbine radius, therefore a high peripheral speed is obtained leading to a good Reynolds number on the blades.

The energy capture is proportional to the swept area and the cube of wind velocity. It is important to identify an equilibrium between energy capture and the cost of the swept area, a bigger area means more manufacturing cost of the turbine. The parameters Φ and ξ are geometric parameters that allow modifying the swept area of the turbine, they are directly related to the design of VAWT turbines.

4.2.4 Number of blades

According to Paraschivoiu [11] for given solidity, it is structurally advantageous to have fewer blades of a larger chord rather than more blades of a smaller chord. This is due to the bending stresses which are dependent on the square of the chord size whereas the aerodynamics loads are dependent on only the first power of the chord. For these reasons, the VAWT have generally two or three blades, but each design is unique for each application, therefore, it's important to analyze the relationship between the geometric parameters as the solidity and the *Cp* of the turbine. **Table 3**, can show some advantages for two and three blades in a VAWT.

4.3 Airfoil selection

The VAWT blades' performance depends largely on the airfoil behavior, which is selected or designed in terms of the wind flow conditions of the feasible location [1].

Employing CFD modeling, Garcia Rodriguez [1] found that the DU06W200 airfoil aerodynamics performance is larger than NACA0018 under the Chicamocha's canyon wind energy conditions. **Table 4** summarizes the calculated

Item	Three blades	Two blades
Construction Cost	Higher	Lower
Assembly Cost	Higher	Lower
Choice of fabrication techniques	Better	Poorer
Strength/Weight ratio	Poorer	Better
Torque ripple	Better	Poorer
Structural dynamics	Better	Poorer

Table 3.
Advantages of two or three blades [11].

Airfoil	Cl	Cd
NACA0018	0.707	0.0801
DU06W200	0.876	0.0853

Table 4.
Lift and drag coefficients of the airfoils NACA0018 and DU06W200 under Chicamocha's canyon wind speed [1].

aerodynamic coefficients of the most feasible point, proving the advantage of considering the DU06W200 airfoil [1].

5. VAWT types and selection

According to Liu et al. [24] the VAWTs are categorized as drag or lift-based devices. The first ones utilize wind drag on the blades to rotate and the last one utilizes the lift on the blades. In **Figure 11** it can observe these categories.

5.1 Drag-based turbines

The Drag-based turbines have the advantage of self-starting ability, and they are commonly found as small-sized turbines in urban and remote areas with relatively low wind speed. These turbines generally are not preferred due to high solidity, heavier weight, and low efficiency. One example of this turbine is the Savonius turbine [24], **Figure 12** shows characteristic parameters of a Savonius wind turbine with two semicircular airfoil blades.

The Savonius turbine produces high torque at low tip-speed ratios (λ) due to the large area facing the wind. The disadvantage with this turbine is that the same drag

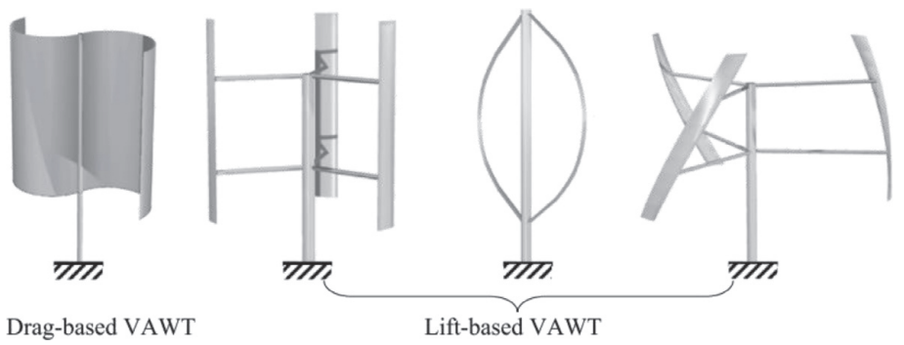

Figure 11.
Schematic view of different types of VAWTs from left to right: S-type Savonius wind turbine, straight-type, Troposkien-type, and helical-type Darrieus wind turbine [24].

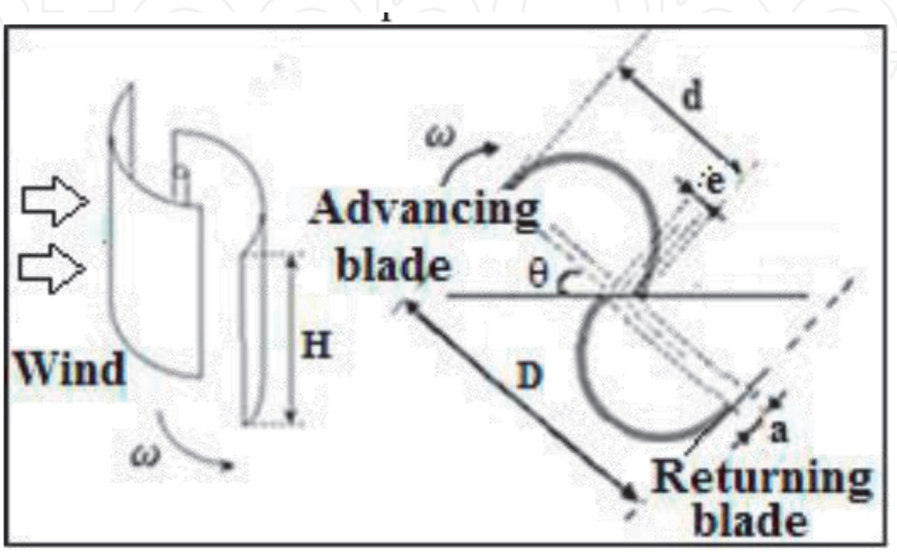

Figure 12.
Two bladed Savonius rotor [25].

of the blades which is used to produce power also works against the turbine by the returning blades, reducing the power that can be obtained [15].

According to Zemamou et al. [25] the number of blades has an important impact on the turbine performance. For obtaining the highest value of the *Cp* under the same test condition, a Savonius turbine must have two blades as shown the **Figure 13**.

5.2 Lift-based turbines

The lift-type turbine consists of airfoil sections that capture the wind energy using the lift force. This lift force produces torque on a shaft, which can then be connected to a generator to produce electricity as power output [15]. The advantage of this configuration is their simple and extruded blades, hence lower manufacturing costs [24]. The straight type, Troposkien type, and helicoidal type are examples of this configuration.

5.2.1 Straight type

These blades usually are used in small-scale, fixed pitch, rooftop designs are commercially available for domestic and other applications. The straight blades have a high value of *Cp* (0.23). This configuration can have any number of blades, from one to a configuration of five. However, the most used are two-bladed (commonly called H-type turbines) or three-bladed [26]. In **Figure 14** it can be the straight blades with two and three blades.

According to Ali and Sattar Aljabair [27] this configuration is better than the type helicoidal at low wind velocity, also, the power coefficient values for DWTs straight model with 2 blades are higher than other models as can see in **Table 5**.

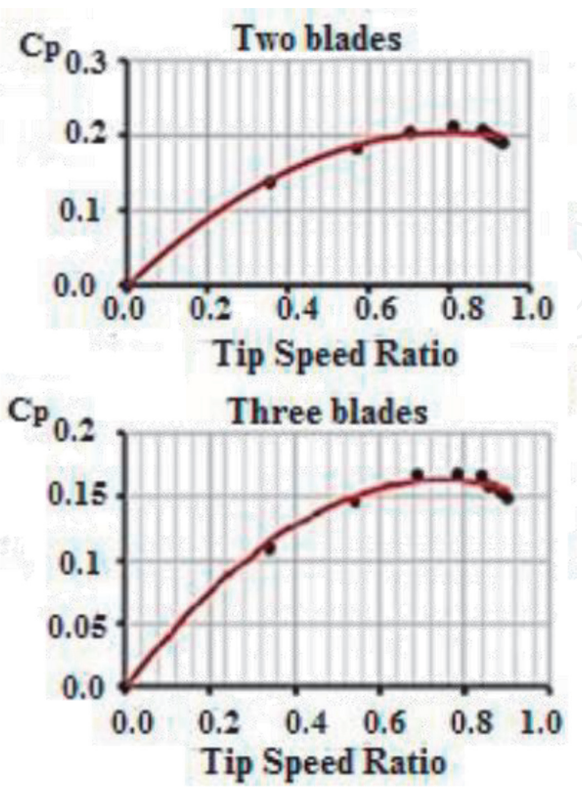

Figure 13.
The Cp variation with the TSR for two & three blades [25].

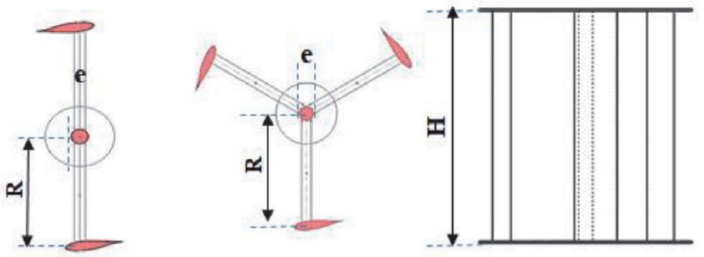

Figure 14.
Darrieus WT type straight blades with two and three blades [27].

DWT type	Number of blades	Wind velocity self-starting (m/s)						
		3	4	4.5	4.85	5.15	6.45	7.65
Straight	2	0.2495	0.2506	0.2635	0.275	0.2895	0.3076	—
	3	0.2407	0.2494	0.2606	0.2678	0.2846	0.3065	—
Twisted 70°	2	0	0	0	0	0.0372	0.0757	0.1216
	3	0	0	0	0.0195	0.0597	0.1008	0.1323
Helical 120°	2	0	0	0	0	0.0449	0.0690	0.0889
	3	0	0	0	0.0427	0.0789	0.1332	0.1465

Table 5.
The (CP) at various wind velocities for DWT models number [27].

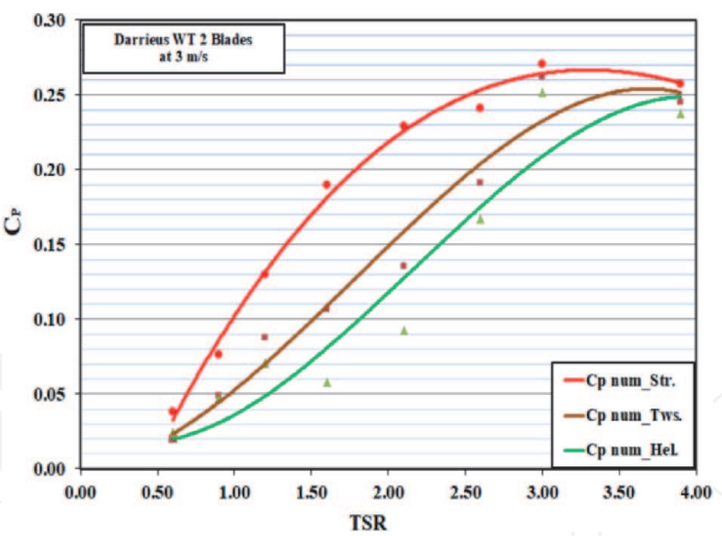

Figure 15.
The numerical relationship between CP and TSR for the DWT models has 2 blades [27].

The Straight blades present a higher value of *Cp* compared to the others as shown the **Figure 15**.

5.2.2 Troposkien

The Troposkien architecture is characterized by hub-to-hub blades, this configuration offers a lower aerodynamic drag (compared to the H-shaped one), which minimizes the bending stress in the blades [28]. In **Figure 16** it can see the Troposkien type.

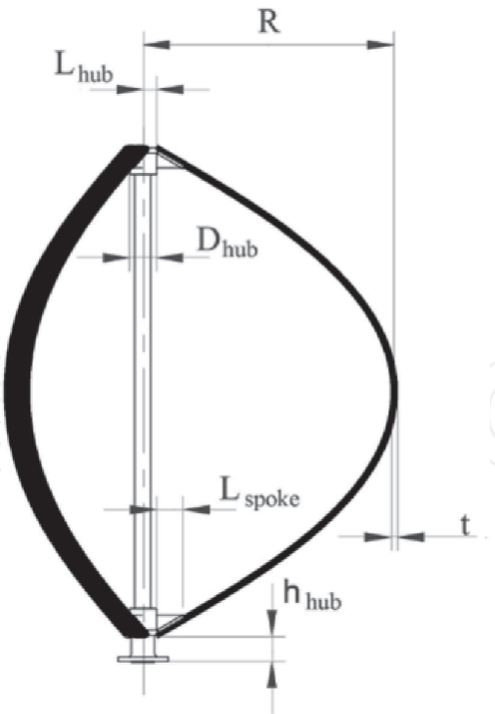

Figure 16.
The Troposkien rotor [28].

According to Battisti et al. [28] the Troposkien type is more efficient than the H-shaped configuration (two straight blades) at high values of TSR as can see in **Figure 17**. On other hand, for low values of TSR, the Troposkien present a lower *Cp* compared to the other type.

Quite similar behavior is registered for low wind velocities and a cut-in wind speed of 6–6.5 m/s is observed. For high values of wind velocity, the Troposkien is capable to generate significantly more power than the H-shaped configuration as shown in **Figure 18**. This quite different behavior could relate to the higher blade Reynolds number, which promotes an improved aerodynamic efficiency, in the investigation of [28], the radius of the Troposkien type is bigger than the H-shaped type to maintain the same rotor swept area. For this reason, the Troposkien type have a bigger Re_c and consequently bigger efficient and more power generated.

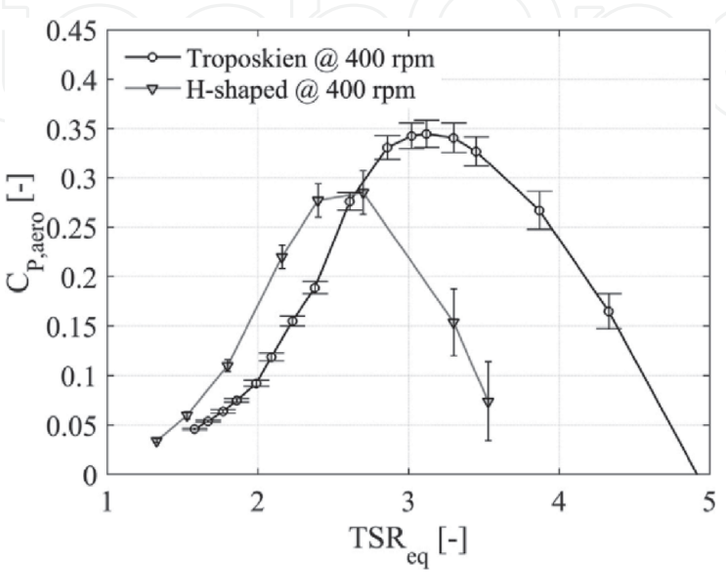

Figure 17.
Rotor power coefficients, as a function of the equatorial tip speed ratio [28].

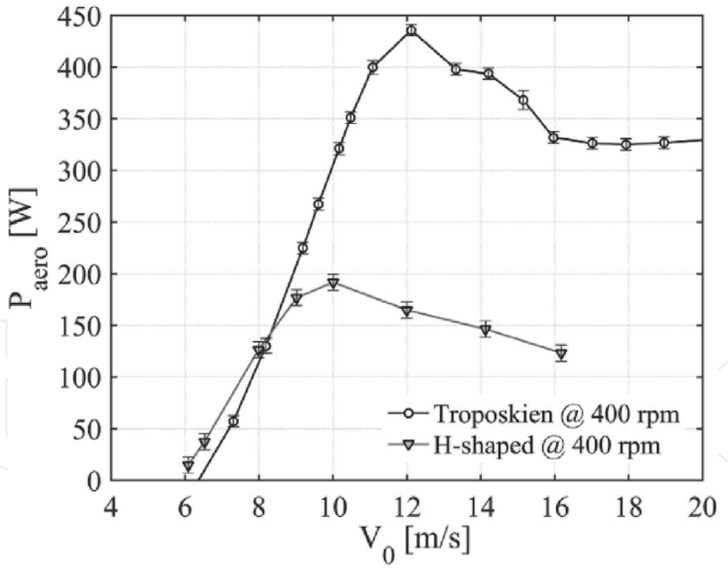

Figure 18.
Power curves for the two analyzed rotor configurations [28].

5.2.3 Helical type

Helical H-rotor distributes the blade airfoil along the rotor perimeter uniformly, thus making the swept area as well as the blade sections constant to the wind in all cases of turbine rotation [29]. In **Figure 19** it can observe the Helical type.

Tjiu et al. [29] made a comparison was made between the helical, straight, and Troposkien types. The comparison was made using 3 blades using the NACA 0015 airfoil with a TSR of 5. The behavior can be seen in **Figure 20** where it can be observed that the Troposkien typology obtained the highest fluctuation with a Cp value of approximately 0.3, the straight blades typology had a fluctuation in the Cp of 0.2 and the lowest fluctuation was obtained by the helicoidal rotor with a variation of approximately 0.03 Cp. However, despite the benefits obtained, the helical blades are more expensive to manufacture, so depending on the desired application

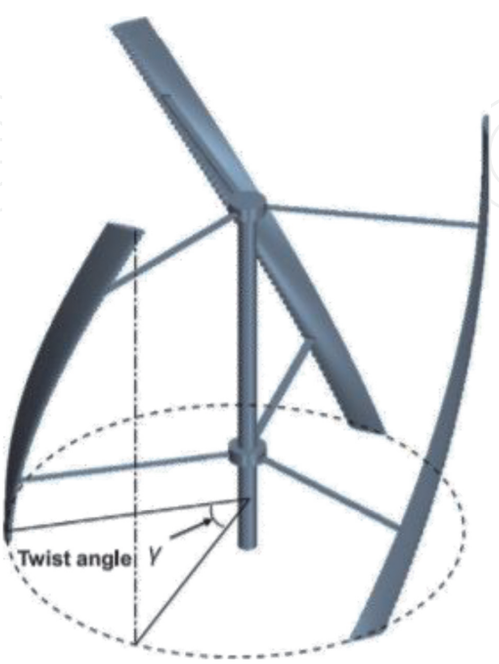

Figure 19.
Helical design [30].

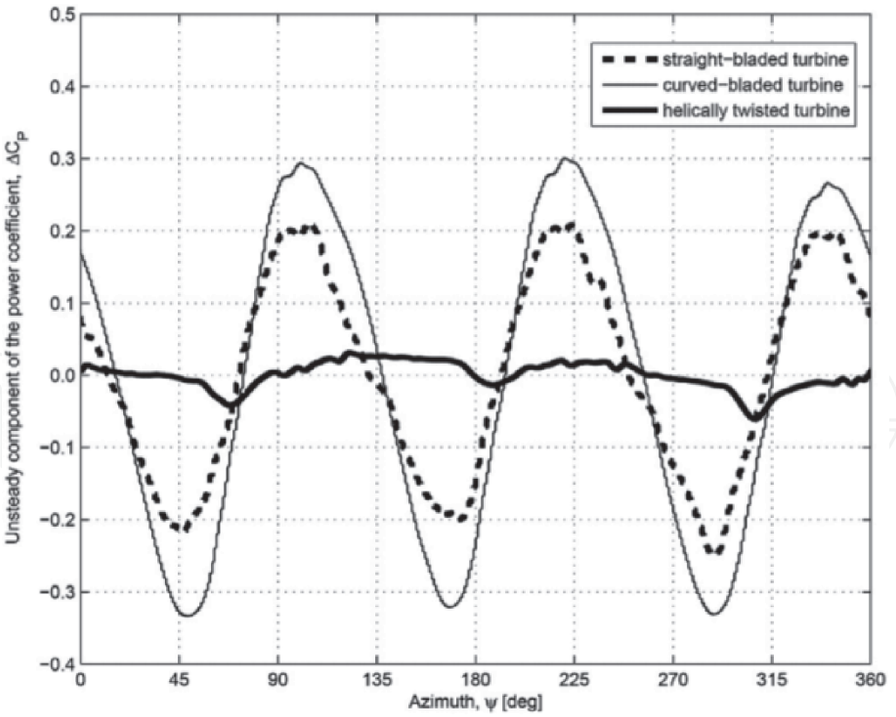

Figure 20.
Power coefficient variations of a typical Troposkien rotor, H-rotor, and helical H rotor.

and the available budget, a middle point must be chosen for the selection of the different types of rotors.

5.3 VAWT selection

A critical factor in the feasibility of power generation with VAWT turbines is the self-starting of the turbine, according to Ali and Sattar Aljabair [27], at a wind speed of 3 m/s, the VAWT with airfoil DU06W200 has the capability of self-starting as seen in **Table 6**. The straight blade type has better performance because the turbine can self-start at lower wind velocity than the others turbines.

The straight blade configuration offers the flexibility to adjust the swept area. Rotor height and diameter can be independently adjusted to suit each design. In addition, this configuration is usually mounted on a tower, which provides higher stability, lower bending, and torsional stresses on the blades compared to the Troposkien topology. Similarly, the gravity-induced bending stress is lower in the straight-bladed configuration as they are stiffer with the same chord length and thickness as the blades of a Troposkien rotor. In addition, they are vertically

DWT type	Number of blades	Wind velocity self-starting (m/s)
Straight	2	3
	3	3
Twisted 70°	2	5.75
	3	5
Helical 120°	2	6.5
	3	6

Table 6.
The wind speed at which Darrieus WT models can be DWT auto-started [27].

Wind speed	Medium	Low
Number of blades N	3	3
Rotor radius R	1 m	3 m
Rotor height H	3 m	5 m
Blade chord c	111 mm	333 mm
Rotor solidity σ	1/3	1/3
Airfoil	DU-06-W-200	DU-06-W-200
Nominal Wind speed	9 m/s	4.5 m/s
Rated power	1.5 kW	1 kW
Maximum power coefficient	0.5798	0.5996

Table 7.
Characteristics of the proposed VAWT designs [13].

positioned and suspended by supports, so they are not subjected to constant bending stress due to gravity [31].

In his investigation Meana-Fernández et al. [13] proposes an optimized design for medium and low wind speed which presents a maximum ?? of 0.5798 and 0.5996 respectively, as observed in **Table 7**.

The type of blades used by [13] were straight blades, it is observed that the proposed design presents a good performance for both medium and low wind speed. It should be noted that for low speeds, as described throughout this section, straight blades perform well without the complexity of construction and high manufacturing cost of the helical type for example, or the instability and torsional stress produced by the Troposkien type.

6. Conclusions

The current literature review analyzes a full VAWT design and installation facility by considering the site wind energy potential, the airfoil performance analysis, and the 3D blade type selection. Experimental and theoretical formulations are referenced to validate the proposed method, leading to an optimal VAWT design. It is found that Chicamocha canyon's large wind energy potential is found at its river, and the critical point is found at one of its boundaries locations ("Mesa de Los Santos"). This wind velocity is taken as a baseline point to select the airfoil and blade designs, as is the minimum value to overcome inertial effects to start VAWT rotation. Literature found that using DU06W200 airfoil, improves by 23% the aerodynamic performance of the VAWT airfoil blades, the reason why is selected to move on at the current design. Finally, the literature review shows that considering 3 straight blades on the VAWT design, complements the airfoil design and selection, as these blades have shown experimentally an accurate performance under the analyzed critical wind flow conditions. The future work will design the size of the VAWT blades and optimized the current proposes, to reach a feasible domain to be used in local facilities.

Conflict of interest

The authors declare no conflict of interest.

Author details

Luis-Fernando Garcia-Rodriguez[1*], Juan Diego Rosero Ariza[2], Jorge Luis Chacón Velazco[2] and Julian Ernesto Jaramillo Ibarra[2]

1 University of São Paulo, Brazil

2 University Industrial of Santander, Colombia

*Address all correspondence to: ingarcia1703@usp.br

References

[1] Garcia Rodriguez LF, Jaramillo JE, Chacon Velasco JL. Chicamocha canyon wind energy potential and VAWT airfoil selection through CFD modeling. Rev Fac Ing Univ Antioquia. 2019;(94):56–66.

[2] Nakano T, Fujisawa N, Oguma Y, Takagi Y, Lee S. Experimental study on flow and noise characteristics of NACA0018 airfoil. J Wind Eng Ind Aerodyn. 2007 Jul;95(7):511–531.

[3] Claessens MC. The design and testing of airfoils for application in small vertical axis wind turbines. Masters Thesis. 2006;1–137.

[4] Yarusevych S, H. Boutilier MS. Vortex Shedding of an Airfoil at Low Reynolds Numbers. AIAA J. 2011 Oct;49 (10):2221–2227.

[5] MANWELL, J.F., McGOWAN JG and RAL. Wind energy explained: theory, design and application. 2nd ed. Wiley; 2009. 677 p.

[6] Manwell J, Mcgowan J, Rogers A. WIND ENERGY EXPLAINED Theory, Design and Application Second Edition. Second. John Wiley & Sons Ltd.; 2009. 689 p.

[7] Bautista H. Control de la calidad de potencia en sistemas de conversión de energía eólica. Las turbinas eólicas. Universidad Nacional de La Plata; 2000.

[8] McLaren K, Tullis S, Ziada S. Measurement of high solidity vertical axis wind turbine aerodynamic loads under high vibration response conditions. J Fluids Struct. 2012;32:12–26.

[9] Brusca S, Lanzafame R, Messina M. Design of a vertical-axis wind turbine: how the aspect ratio affects the turbine's performance. Int J Energy Environ Eng. 2014;5(4):333–340.

[10] Hansen JT, Mahak M, Tzanakis I. Numerical modelling and optimization of vertical axis wind turbine pairs: A scale up approach. Renew Energy [Internet]. 2021;171:1371–81. Available from: https://doi.org/10.1016/j.renene.2021.03.001

[11] Paraschivoiu I. Wind Turbine Design: With Emphasis on Darrieus Concept. Schettini S, editor. Presses Inter Polytechnique. Montreal: Presses Internationales Polytechnique; 2002. 1–438 p.

[12] Edwards J. The Influence of Aerodynamic Stall on the Performance of Vertical Axis Wind Turbines [Internet]. The University of Sheffie; 2012. Available from: http://etheses.whiterose.ac.uk/2722/

[13] Meana-Fernández A, Solís-Gallego I, Fernández Oro JM, Argüelles Díaz KM, Velarde-Suárez S. Parametrical evaluation of the aerodynamic performance of vertical axis wind turbines for the proposal of optimized designs. Energy. 2018;147:504–517.

[14] Mohamed MH. Impacts of solidity and hybrid system in small wind turbines performance. Energy. 2013;57:495–504.

[15] Mohamed MH. Impacts of solidity and hybrid system in small wind turbines performance. Energy [Internet]. 2013;57:495–504. Available from: http://dx.doi.org/10.1016/j.energy.2013.06.004

[16] Zouzou B, Dobrev I, Massouh F, Dizene R. Experimental and numerical analysis of a novel Darrieus rotor with variable pitch mechanism at low TSR. Energy [Internet]. 2019;186:115832. Available from: https://doi.org/10.1016/j.energy.2019.07.162

[17] Elkhoury M, Kiwata T, Aoun E. Experimental and numerical investigation of a three-dimensional

vertical-axis wind turbine with variable-pitch. J Wind Eng Ind Aerodyn [Internet]. 2015;139:111–123. Available from: http://dx.doi.org/10.1016/j.jweia.2015.01.004

[18] Marinić-Kragić I, Vučina D, Milas Z. Numerical workflow for 3D shape optimization and synthesis of vertical-axis wind turbines for specified operating regimes. Renew Energy. 2018;115:113–127.

[19] Posa A. Influence of Tip Speed Ratio on wake features of a Vertical Axis Wind Turbine. J Wind Eng Ind Aerodyn [Internet]. 2020;197(April 2019):104076. Available from: https://doi.org/10.1016/j.jweia.2019.104076

[20] Bianchini A, Ferrara G, Ferrari L. Design guidelines for H-Darrieus wind turbines: Optimization of the annual energy yield. Energy Convers Manag [Internet]. 2015;89:690–707. Available from: http://dx.doi.org/10.1016/j.enconman.2014.10.038

[21] Islam M, Ting DSK, Fartaj A. Aerodynamic models for Darrieus-type straight-bladed vertical axis wind turbines. Renew Sustain Energy Rev. 2008;12(4):1087–1109.

[22] Rathore MK, Agrawal M, Baredar P. Materials Today : Proceedings Energy production potential from the wake of moving traffic vehicles on a highway by the array of low economic VAWT. Mater Today Proc [Internet]. 2020;(xxxx). Available from: https://doi.org/10.1016/j.matpr.2020.08.638

[23] Bianchini A, Ferrara G, Ferrari L. Design guidelines for H-Darrieus wind turbines: Optimization of the annual energy yield. Energy Convers Manag. 2015;89:690–707.

[24] Liu J, Lin H, Zhang J. Review on the technical perspectives and commercial viability of vertical axis wind turbines. Ocean Eng [Internet]. 2019;182(October 2018):608–26. Available from: https://doi.org/10.1016/j.oceaneng.2019.04.086

[25] Zemamou M, Aggour M, Toumi A. Review of savonius wind turbine design and performance. Energy Procedia [Internet]. 2017;141:383–8. Available from: https://doi.org/10.1016/j.egypro.2017.11.047

[26] Aslam Bhutta MM, Hayat N, Farooq AU, Ali Z, Jamil SR, Hussain Z. Vertical axis wind turbine - A review of various configurations and design techniques. Renew Sustain Energy Rev. 2012;16(4):1926–1939.

[27] Ali, Nawfal M., Sattar Aljabair AHA. An Experimental and Numerical Investigation on Darrieus Vertical Axis Wind Turbine Types at Low Wind Speed. Int J Mech Mechatronics Eng. 2019;19(December 2019):97–110.

[28] Battisti L, Persico G, Dossena V, Paradiso B, Raciti Castelli M, Brighenti A, et al. Experimental benchmark data for H-shaped and troposkien VAWT architectures. Renew Energy. 2018;125:425–444.

[29] Tjiu W, Marnoto T, Mat S, Ruslan MH, Sopian K. Darrieus vertical axis wind turbine for power generation I: Assessment of Darrieus VAWT configurations. Renew Energy. 2015;75:50–67.

[30] Wang Z, Wang Y, Zhuang M. Improvement of the aerodynamic performance of vertical axis wind turbines with leading-edge serrations and helical blades using CFD and Taguchi method. Energy Convers Manag [Internet]. 2018;177(May):107–21. Available from: https://doi.org/10.1016/j.enconman.2018.09.028

[31] Tjiu W, Marnoto T, Mat S, Ruslan MH, Sopian K. Darrieus vertical axis wind turbine for power generation I: Assessment of Darrieus VAWT configurations. Renew Energy. 2015;75:50–67.